Size Distribution of Inorganic Elements in Bottom Ashes from Seven Types of Bio-fuels across Beijing-Tianjin-Hebei Region, China

Zhiyong Li[1*], Huiqiao Ma[1], Fan Lin[1], Peng Zhao[1], Lei Wang[2], Yunjun Jiang[2], Caixiu An[2], Aiqin Liu[2], Zishu Hu[3], Hui Jin[4]

[1]*School of Environmental Science and Engineering, North China Electric Power University, Baoding 071000, China*

[2]*Central Laboratory of Geology and Mineral Resources of Hebei Province, Baoding 071003, China*

[3]*Electric Power Research Institute of State Grid Xinjiang Electric Power Company, Urumqi 830000, China*

[4]*M&T Center of EHV Power Transmission Company of CSG, Guangzhou 510663, China*

ABSTRACT

A total of fifty-six bottom ash (BA) samples from indoor burning of seven bio-fuels (BFs) using Zaotai stove were collected from eight sampling sites across Beijing-Tianjin-Hebei (BTH) region from April to December, 2016. Each one was divided into six parts as PM_{+148}, $PM_{93–148}$, $PM_{67–93}$, $PM_{53–67}$, $PM_{40–53}$ and $PM_{–40}$ using vibrating screen. The lower sized three parts including $PM_{53–67}$, $PM_{40–53}$ and $PM_{–40}$ were selected for analysis of 39 inorganic elements (IEs) using ICP-MS and ICP-OES. The firewood–walnut (WAL) had the lowest ash yield as 34.3±3.55 g kg^{-1}, the corresponding values for 6 crop straws were millet (MIL) >sorghum (SOR)> sesame (SES)> corn (COR)> cotton (COT)> soybean (SOY). The ash yields were generally positive correlated the particle sizes of BAs for seven BFs. The eight top elements (TEs) including Si, Ca, Mg, K, P, Al, Na and Ti dominated in all BAs regard less of their fluctuation among seven BFs and Σ_8TEs were well correlated with Σ_{39}IEs (R^2=0.99, p<0.001). The Σ_{39}IEs were not correlated with particle size of BAs due to significantly fluctuation of 8 TEs. The trace elements including Sc, Li, P, V, Cr, Co, Ni, Sb, As, Y, Cs, Bi, Tl, Th, Sn, Cd, La, Ce, Sm, W and U were well negative correlated with particle size of BAs from 7 BFs, while the 8 TEs with higher content except for Al showed not this trend. The heavy metal (HM) profiles were similar between any two sized BAs for all the seven BFs based on lower values of coefficient of divergence (CD). The 6 pairs of BFs out of 21 pairs of BFs were different in HM profiles based on higher CD values. The HMs including Zn, Cu, Pb, V, Cr and Ni had the higher levels among seven BFs. The contents of V in BAs from COR were beyond the limits designated by European countries for BAs used as soil conditioner. The enrichment factors (EFs) of 12 HMs were not correlated particle sizes of BAs, resulted from the fluctuation of Al used as reference element among different sized BAs. The HMs as Cu, Zn, Cd, Sn had higher EFs more than 10 indicated they were significantly influenced by human activities.

Keywords: Bio-fuel; Bottom ash; Heavy metal; Inorganic element; Beijing-Tianjin-Hebei

---

[*]Corresponding author.

Tel.: +86 312 7525506; Fax: +86 312 7525506

ACCEPTED MANUSCRIPT

E-mail address: lzy6566@126.com

INTRODUCTION

Biomass burning (BB) was widely known as open burning of any non-fossilized agricultural residues, grass and forest, and residential combustion of BFs for cooking and heating (Engling *et al.*, 2014). It is the largest source of fine carbonaceous particles and the second largest trace gases such as SO_2, NO_x, NMVOCs, NH_3, could affect on atmospheric chemistry, global climate and human health (Arola *et al.*, 2007; Liu *et al.*, 2013; Popovicheva *et al.*, 2015; Tian *et al.*, 2015; Lee *et al.*, 2016; Zhu *et al.*, 2016; Li *et al.*, 2017; Ommi *et al.*, 2017). Bond *et al.* (2004) also reported BB was the largest source of primary organic carbon (POC) and element carbon (EC) in the world. The serious atmospheric pollution attributed to various pollutants from BB were reported frequently (Eckhardt *et al.*, 2007; Alves *et al.*, 2010; Kondo *et al.*, 2011; Engling *et al.*, 2014). Some studies revealed fine particles can cause adverse health effects such as pulmonary function failure, respiratory diseases and lung cancer (Huang *et al.*, 2012; Shi and Yamaguchi, 2014; Zhou *et al.*, 2017). The toxic pollutants adsorbed and absorbed in emitted particles from BB such as heavy metals and organic compounds could result in seriously adverse health effects (Habeebullah, 2016; Wei *et al.*, 2016; Li *et al.*, 2017).

The people relying on the traditional use of biomass for cooking and heating was predicted to rise from 2.7 billion today to 2.8 billion in 2030 around the world (UNDP, 2002). In China, the annual straw burning capacity was as high as 140 Tg and accounted for 23.3% of total crop products, especially in eastern and northeastern China (Cao *et al.*, 2008). BB as renewable energy was commonly used in Chinese rural areas and domestic BB was the most prevailing utility in China (Wang *et al.*, 2009; Zhou *et al.*, 2017). During combustion process, the IEs stored in biomass and soil for a long time emitted again into atmosphere and subsequently transported to other areas (Eckhardt *et al.*, 2007). The re-emission of radioactive cesium-137 and mercury from biomass burning were documented (Wotawa *et al.*, 2006; Sigler *et al.*, 2003). The much more BAs compared with fly ashes produced from BB were not properly treated and always casually dumped in China. It was a fact can't be ignored the pollutants in dumped BAs could enter into soil and atmosphere by wind strength. But few comprehensive studies on emitted element characteristics in BAs from indoor BB were conducted in China.

As a cultural and political center of China and economic center of northern China, BTH suffered extreme and frequent haze episodes caused by rapid economic growth and urbanization (Zhang *et al.*, 2017). Two cities in Hebei province as Baoding and Shijiazhuang were ranked as 1st and 2nd most polluted cities in China (Balasubramanian *et al.*, 2017). Annual $PM_{2.5}$ level of BTH in 2014 was 6.2 and 2.7 times as much as the corresponding values appointed by Chinese Class I and Class II standards (Chen *et al.*, 2017). Some studies reported the BB contributed 35-50% of fine particles to

ACCEPTED MANUSCRIPT

Beijing atmosphere. Consequently, it is of great importance to clarify the pollution characteristic of heavy metals in BAs from BB.

Zaotai stove is a typical burning tool for indoor BB in BTH. In this study, 8 sites across BTH were selected to collect BAs for 7 BFs from Zaotai stove and the main aims were to investigate: 1) influence of BF types on elemental compositions in BAs from BTH; 2) size distribution of IEs for 7 BFs; 3) similarity comparison of heavy metal profiles among different BFs or BAs with different sizes for each BF.

BOTTOM ASH SAMPLING AND ELEMENT ANALYSIS

Sampling Area Description and Bottom Ash Sampled

Beijing-Tianjin-Hebei (BTH) region (36.07°N–42.65°N and 113.46°E–119.79°E) locates in North China plain, which includes 2 municipalities (Beijing and Tianjin) and 11 prefecture-level cities of Hebei province, covers an area of 216,500 km^2 and has 110,000,000 people. BTH is the most important and dynamic economic zone in northern China, but also is the most air polluted zone (Zhang *et al*., 2017; Chen *et al*., 2017). Although BAs were indirectly entered into air, but it could entered into air by wind power after dumped carelessly. To our knowledge, few studies were conducted on BB across BTH.

In this study, 8 sites including Beijing, Tianjin and other 6 prefecture-level cities such as Tangshan, Xingtai, Zhangjiakou, Chengde, Baoding and Shijiazhuang were selected to collected BA samples for 7 BFs from Zaotai stoves **(Fig. 1)**. The 56 BAs were vibration screened using vibration sieve (Xinxiang Beiteli Vibration Machine LTD.) into 6 different sized parts. Finally the lower sized 3 parts including $PM_{53–67}$, $PM_{40–53}$ and $PM_{–40}$ were selected for 7 BFs for analysis of 39 IEs because the finer parts were more easily enter into atmosphere compared with the coarse parts. All crop straw and firewood samples were dried using a vacuum freeze dryer, and then stored in brown glass bottles before analysis in order to eliminate the influence of water.

(Fig. 1)

Sample Pre-treatment and Element Analysis

The elements in BAs were analyzed using combination of ICP-MS system (Agilent 7700X, Agilent Co. USA) and ICP-OES system (VISTA-MPX, Varian Co. USA). The 30 of 39 IEs such as Li, Be, Na, P, K, Sc, V, Cr, Mn, Co, Ni, Cu, Zn, As, Rb, Y, Mo, Cd, Sn, Sb, Cs, La, Ce, Sm, W, Tl, Pb, Bi and Th were analyzed by ICP-MS and the other 9 ones such as Si, Al, Ca, Mg, Fe, Ti, Ba, Sr and Zr were

ACCEPTED MANUSCRIPT

analyzed by ICP-OES. The same analysis method was selected in this study as Li *et al*. (2017).

The method was described briefly as followed: 1) For ICP-MS, 0.2000 g BA was heated together with 5 mL of aqua regia and 1 drop of HF acid until evaporated to dryness. Then was heated for 20 min with 2% of HCl acid and the extract was transferred into a plastic comparison tubes waiting for analysis. 2) For ICP-OES, 0.1000 g of BA was transferred into a Teflon crucible and heated using a muffle furnace, and then gradually heated up to 530–550 ℃ for completely ashing. The absolute ethanol and NaOH powder were added and heating again at 500 ℃ for 10 min in a muffle furnace. It was subsequently boiled together with added water on an electric heating plate. The HCl acid was added and transferred into a PVC colorimetric tube and diluted to 10 mL waiting analysis.

For 30 IEs analyzed using ICP-MS, the method detection limits (MDLs) (reported in $\mu g\ g^{-1}$) were in the range of 0.001 (e.g. MDLs of Bi, Th, U, Tl, Be, Sc and Cs) to 10.3 of K with the mean value as 0.665±2.25, while they were ranged from 0.004 of Sr to 1.81 of Fe with the mean value as 0.459±0.559 for 9 IEs analyzed using ICP-OES. All the relative standard deviation (RSD) values for 39 IEs were lower than 5%, they were 2.11%, 2.87%, 3.45%, 2.83%, 1.97%, 3.95%, 3.23%, 4.52%, 4.25%, 3.21%, 2.51%, 2.77%, 4.56%, 1.87%, 2.96%, 3.29%, 4.55%, 2.60%, 3.35%, 2.59%, 2.89%, 3.47%, 4.73%, 4.69%, 2.94%, 2.96%, 2.71%, 2.64%, 3.71%, 3.28%, 4.11%, 4.21%, 3.01%, 2.01%, 2.71%, 3.17%, 2.99%, 4.05% and 3.65% for Li, Be, Na, P, K, Sc, V, Cr, Mn, Co, Ni, Cu, Zn, As, Rb, Y, Mo, Cd, Sn, Sb, Cs, La, Ce, Sm, W, Tl, Pb, Bi, Th, Si, Al, Ca, Mg, Fe, Ti, Ba, Sr, Zr and U, respectively. The recoveries for 39 analyzed IEs using analysis method adopted in this study were in the range of 85-115%.

Standard soil materials (SSMs) as GBW07446-GBW07457 (Center for National Standard Matter, China) were used to assess the accuracy of ICP-MS and ICP-OES. The background contamination was routinely assessed using process and solvent blank experiments. The standard materials were analyzed every 5 BA samples to evaluate the instrument repeatability. One BA sample was repeated analyzed every 6 samples with the RSD values were lower than 15%.

RESULTS AND DISCUSSION

Size Distribution of Ash Yields for Seven BFs

The BA samples were vibration screened into 6 parts and weighed to obtain the corresponding ash yield values. **Fig. 2a** showed the size distribution of ash yields for 7 BFs. In generally, ash yields for all the 7 BFs showed the positive correlation with particle sizes. PM_{+148} accounted for the highest proportion of total ash amounts and PM_{-40} had the lowest corresponding values for all the 7 BFs. The percentage of PM_{+148} in total ash amounts were ranged from 33.53±4.12% for WAL to 66.02±5.26%

ACCEPTED MANUSCRIPT

for SES, while the corresponding values for PM_{-40} were in the range of 0.84±0.112% for SOY to 5.89±0.652% for COT. The sum of ashes for 3 lower sized parts including $PM_{53–67}$, $PM_{40–53}$ and PM_{-40} were ranged from 7.91±0.521% (WAL) to 22.05±3.123% (COR) of the total ash yields.

The BA amounts (reported in ash g kg^{-1} BF) produced from BB varied significantly among 7 BFs, they were decreased as MIL (136±18.5 g kg^{-1}) > SOR (72.4±9.52 g kg^{-1}) > SES (72.0±8.88 g kg^{-1}) > COR (44.8±3.99 g kg^{-1}) > COT (42.2±2.98 g kg^{-1}) > SOY (40.0±3.52 g kg^{-1}) >WAL (34.3±3.55 g kg^{-1}) **(Fig. 2b)**. The firewood as WAL had the lowest ash yield compared with the other 6 crop straws due to its more thoroughly burning.

(Fig. 2.)

Contents of Individual Elements in BAs

Total contents of 39 inorganic elements (Σ_{39}IEs) (in mg g^{-1}) were ranged from 0.249±0.021 ($PM_{40–53}$ from WAL) to 0.493±0.036 ($PM_{53–67}$ from SES) with the mean value as 0.412±0.071 for 7 BFs **(Fig. 3a)**. The top elements (TEs) including Si, Ca, Mg, K, P, Al, Na and Ti dominated in BB samples for all 7 BFs regardless of their contents varied significantly among different BFs (Table 1a). The Σ_{39}IEs were not correlated with particle size of BAs for 7 BFs due to obvious fluctuation of 8 TEs among 7 BFs. The sum of these 8 TEs (Σ_8TEs) (mg g^{-1}) for all sized BAs from 7 BFs were ranged from 0.247±0.021 ($PM_{40–53}$ from WAL) to 0.491±0.032 ($PM_{53–67}$ from SES). The Σ_8TEs accounted for 98.76% of Σ_{39}IEs for $PM_{53–67}$ from WAL to 99.48% of Σ_{39}IEs for $PM_{53–67}$ from SOR. Fig. 2b showed that Σ_8TEs for all BAs were well correlated with the corresponding Σ_{39}IEs (R^2=0.99, p<0.001) **(Fig. 3b)**.

(Fig. 3)

(Table 1a)

These TEs varied significantly not only among different BFs, but also among different sized BAs for the same BF. For $PM_{53–67}$ among 7 BFs, the contents for 8 TEs followed as K> Ca> P> Si> Mg> Fe> Al for COT, while they were Si> K> Ca> Mg> P> Fe> Al, Si> Ca> K> Fe> P> Al> Mg, Si> Ca> K> Mg> Fe> P> Al, Ca> Si> K> P> Al> Mg> Fe, K> Ca> Al> Mg> Si >P >Fe, and K> Ca> Si> Mg>

ACCEPTED MANUSCRIPT

P> Al> Fe for COR, MIL, WAL, SOR, SOY and SES, respectively. The contents of Na were higher than those of Ti for all the 7 BFs (Table 1a). The combustion of different BFs resulted in different element compositions. Hasan *et al*. (2009) reported the similar result with Pb, Hg, Fe and Ca were dominated in BAs from rice husk combustion, while Pb, Fe and Mg dominated in BAs from a mixed BF (straw, bamboo, cow dung, leaves and plants). Wang *et al*. (2016) reported the main elements were also K, Ca, P and Mg in BAs from burning of straws of corn, wheat and rice due to they were essential ones for plant growth.

K was often used as identification element for biomass burning (Duan *et al*., 2004). In this study, the content of K varied significantly among 7 BF from different sampling sites, possibly resulted from the difference of plant physiological characteristics and local soil characteristics among different sites in BTH (Wang *et al*., 2016; Duan *et al*., 2004). Consequently the use of K identification element should be cautioned in BTH.

It should be noted, the IEs were classified into 3 classes according to their relationship with particle sizes: 1) IEs with higher contents (e.g. Si, Ca, K, Mg, Fe, P and Ti) except for Al were not correlated with particle size for all the 7 BFs, Al was well correlated with particle size of BAs from 7 BFs; 2) IEs with lower contents (e.g. Sc, Li, P, V, Cr, Co, Ni, Sb, As, Y, Cs, Bi, Tl, Th, Sn, Cd, La, Ce, Sm, W and U) were well negative correlated with particle size for all the 7 BFs; 3) IEs with medium content (e.g. Mn, Na, Zn, Cu, Sr, Zr, Rb, Pb and Mo) within partial BFs showed the well correlation relationship **(Table 1a–c)**. For examples, Pb within 5 of 7 BFs were well correlated with particle size of BAs such as COT, MIL, WAL, SOY and SES, while Mn within only 2 of 7 BFs showed this trend such as COR and MIL. Li *et al*. (2017) reported the 39 IEs except for Cu within fly ashes emitted from 15 Chinese power plants were more inclined to enrich in finer particles as $PM_{2.5}$. These differences possibly resulted from the different ash characteristics, combustion conditions, fuels and combustion devices.

Suitability Assessment of Application of Bottom Ashes as Soil Conditioner

The exposure of people to heavy metals (HMs) would pose serious adverse health effects (Zheng *et al*., 2016). Cr and Mn abounded in particles could result in acute and chronic damage of lung (Zheng *et al*., 2013). Cr and Cd were strongly carcinogenic elements regardless of their low contents (Zheng *et al*., 2016).

In this study, 12 HMs (e.g. Fe, Mn, Cu, Zn, Cr, Cd, Sn, Co, As, Pb, V and Ni) most concerned by people were all detected. The HMs including Mn and Fe dominated among all the BAs. The HMs including Zn, Cu, Pb, V, Cr and Ni had higher levels among all BAs **(Table 1a and c).** Saqib and Bäckström. (2016) also reported Zn, Cu and Pb were predominant HMs in fly ashes from combustion of 13 BFs, while Lanzerstorfer, (2015) reported the top HMs in fly ashes from 8 Australian grate-fired BB plants were Zn, Pb and Cr. Although the content order was similar, the contents of corresponding

ACCEPTED MANUSCRIPT

HMs were much lower than those of fly ashes from biomass burning. The volatile HMs would rather enrich in finer fly ashes compared to coarser BAs possibly be the explanation (Lanzerstorfer, 2015).

In Australia, BAs from BB were widely used as soil conditioner if the contents of contained HMs were below the corresponding threshold values, while fly ashes were prohibited for that utility way due to higher contents of contained HMs (Lanzerstorfer, 2015). Emilsson. (2006) and Stupak *et al.* (2008) reported the limits (in mg kg^{-1}) of HMs such as As, Cr, Cd, Cu, Hg, Ni, Pb, V and Zn designated by two European countries, they were 30, 30, 100, 400, 3, 70, 300, 70 and 7000 for Sweden, and 30, 30, 100, 400, 3, 70, 300, 70 and 7000 for Lithuania, respectively.

In this study, the contents (in mg kg^{-1}) of Pb ranged from 4.27±0.65 ($PM_{53–67}$ from SOY) to 28.3±5.26 ($PM_{53–67}$ from COR), and V ranged from 6.03±1.02 ($PM_{53–67}$ from WAL) to 81.1±9.25 ($PM_{–40}$ from COR). Cd had the lowest contents ranged from 61.5±6.22 ng g^{-1} ($PM_{53–67}$ from WAL) to 610±85.6 ng g^{-1} ($PM_{–40}$ from COR) **(Table 1c)**. Among 12 HMs in all sized BAs from 7 BFs, only V in COR exceeded the limit of 70, so the application of COR BAs in BTH as soil conditioner should be prohibited.

(Table 1a–c)

Similarity Comparison of Heavy Metal Profiles

As a receptor model, chemical mass balance (CMB) model was often used to the work of source apportionment of atmospheric pollutants for different regions (Kong *et al.*, 2011). The source profiles for different emission sources were urgently needed for CMB calculation, while the establishment of source profiles was a heavy work (Li *et al.*, 2017). The similarity of element profiles among different BFs or different sized BAs within one BF would make they can be replaced each other and consequently reduced workload of establishment of source profiles (Li *et al.*, 2017).

A parameter as coefficient of divergence (CD) was commonly used to compare the similarity of pollutant profiles emitted from different sources (Wongphatarakul *et al.*, 1998; Kong *et al.*, 2011; Li *et al.*, 2016, 2017). A threshold of CD as 0.3 was often used to identify the similarity of pollutant profiles of source j and k, less than 0.3 indicated pollutant profiles between j and k were similar, higher than 0.3 suggested they were different, while 0 and 1 indicated they were completely same and different, respectively (Wongphatarakul *et al.*, 1998). Kong *et al.* (2011) reported the PAH profiles for six stationary sources in a Chinese oilfield city-Dongying were similar based on lower CD values (lessen than 0.3).

ACCEPTED MANUSCRIPT

Source apportionment of atmospheric particle bounded HMs was more concerned due to their serious threat to human health. The CD values for HM profiles among any 2 out of 7 BFs and among any 2 different sized BAs within one BF were calculated as followed:

$$CD_{jk} = \sqrt{\frac{1}{p}\sum_{i=1}^{p}\frac{\left(x_{ij} - x_{ik}\right)^2}{\left(x_{ij} + x_{ik}\right)^2}} \qquad (1)$$

Where p was the number of analyzed HMs and it was 12 in this study, j and k were emission sources of HMs (they were BA samples from 7 BFs or different sized BAs from the same BF in this study), x_{ij} and x_{ik} were mass percentage of element i within j and k (Wongphatarakul *et al*., 1998; Li *et al*., 2016, 2017).

The CD values between any 2 sized BA samples within one BF were listed in Table 2. All the CD values were lessen than 0.3 and they were ranged from 0.025±0.015 ($PM_{53–67}$ *vs* $PM_{40–53}$ within COT) to 0.259±0.012 ($PM_{53–67}$ *vs* $PM_{–40}$ within WAL) with the mean value as 0.144±0.068, indicated HM profiles between any 2 sized BAs within each one of 7 BFs were similar **(Table 2)**. Consequently the HM profiles for different sized BAs within one BF were similar and could be replaced each other.

(Table 2)

Due to the similarity of HM profiles between any 2 sized BAs for one BF, HM profile of $PM_{53–67}$ was appointed to represent the corresponding profile for whole BF. CD values were calculated based on 12 HMs for any 2 BFs and the results were listed in Table 3. In generally, the CD values between any 2 BFs were higher than those between any 2 sized BAs within one BF. Except for 6 bold numbers, the other 15 CD values were all lessen than 0.3 **(Table 3)**. The highest CD value of 0.467±0.067 occurred at COR vs SOY and the lowest one as 0.153±0.023 occurred at MIL vs SOR. The bold numbers higher than 0.3 suggested the source profiles for these sources were different each other. The HM profile of COT were similar with those of the other 6 BFs based on 6 CD values lessen than 0.3. WAL was similar to HM profiles of 5 BFs except for SES. SOR was similar to those of 5 BFs except for SES. COR was similar to those of 4 BFs except for SOY and SES. MIL was similar to those of 4 BFs except for SOY and SES.

(Table 3)

ACCEPTED MANUSCRIPT

Enrichment Factors of Heavy Metals in all BAs

The enrichment factor (EF) was widely used to identify the element was originated from human activities or natural process, and then assess the content of anthropogenic influence. The element was mainly crustal origin if it's EF close to 1, while EF higher than 10 suggested significant influence of human activities (Li *et al*., 2013). In this study, EF was used to assess the influence of casually dumped BAs on its receptor soil or air. The EF was calculated based on following equation:

$$EF = (C_n / C_{ref}) / (B_n / B_{ref}) \qquad (2)$$

Where C_n is measured content of element in BA, B_n is background content of element in soil from BTH, C_{ref} and B_{ref} is measured content and background content of reference element in BA and BTH soil. Although the utility of different reference elements would result in the different EF values, Al was often used as reference element in Chinese related studies (Hao *et al*., 2009; Zhang *et al*., 2010). So Al was chosen as reference element accordingly in this study.

Fig. 4 showed the EFs for 12 HMs in different sizes BAs from 7 BFs. The EFs for 12 HMs varied significantly among different BFs and were not correlated with particle size of BAs for all the 7 BFs. The EFs for Cu and Zn were higher than 10, indicated the significant influence of dumped BAs on receptor soil. The highest EF as 69.1 for Cu occurred at $PM_{53–67}$ from SOY.

For 12 HMs, Cu, Zn, Cd, Sn and Pb had higher EFs among all the 7 BFs (**Fig. 4**). The EFs for HMs varied significantly among different BFs. For examples, Cu was more inclined to enrich in SOY, while As and Pb were more enriched in COT.

All the EFs for 12 HMs among 7 BFs showed not correlated with particle size of BAs regard less of their contents had well correlation with particle sizes, which was resulted from varied Al contents among different sized BAs.

(Fig. 4)

CONCLUSIONS

The BA samples were collected for 7 BFs from each one of 8 sampling sites across BTH region. So 56 BA samples were obtained and every BA sample was divided into 6 parts with different sizes. The 3 parts with lower particle sizes for 56 BAs including $PM_{53–67}$, $PM_{40–53}$ and $PM_{–40}$ were collected for analysis of 39 IEs using ICP-MS and ICP-OES. The Σ_{39}IEs (reported in mg g^{-1}) ranged from 0.249±0.021 to 0.493±0.036 with the mean value as 0.412±0.071 for 7 BFs. The IEs including K, Ca,

ACCEPTED MANUSCRIPT

Si, P, Fe, Al, Na and Ti dominated in the BAs regard less of their contents varied significantly among all the 7 BFs. The predominant IEs including Si, Ca, K, Mg, Fe, P and Ti except for Al were not correlated with particle size of BAs for all the 7 BFs, while the trace IEs including Sc, Li, P, V, Cr, Co, Ni, Sb, As, Y, Cs, Bi, Tl, Th, Sn, Cd, La, Ce, Sm, W and U were well negative correlated with particle size of BAs for all the 7 BFs. All the BAs except for V in COR had the HM contents lessen than those designated by European standard values used as soil conditioner, BAs from COR should be prohibited in BTH.

The HMs including Zn, Cu, Pb, V, Cr and Ni had higher levels among all BA samples from 7 BFs. All the CD values for 12 HMs between any two size ranged BAs for the same BF were lessen than 0.3 indicated the similarity of HM profiles for different sized BAs from one BF. The CD values for 12 HMs between 6 of 21 pairs of BFs were higher than 0.3 indicated different HM profiles exist among some BFs. The HMs including Cu, Zn, Cd, Sn and Pb had the higher EF values for all the 7 BFs. The EF values for Cu, Zn, Cd and Sn were higher than 10 suggested the significant influence of human activities.

ACKNOWLEDGEMENT

This study was supported by National Natural Science Foundation of China (21407048) and the Fundamental Research Funds for the Central Universities (2017MS142).

REFERENCES

Alves, C.A., Gonçalves, C., Pio, C.A., Mirante, F., Caseiro, A., Tarelho, L., Freitas, M.C. and Viegas, D.X. (2010). Smoke emissions from biomass burning in a Mediterranean shrubland. *Atmos. Environ*. 44:3024–3033.

Arola, A., Lindfors, A., Natunen, A. and Lehtinen, K.E.J. (2007). A case study on biomass burning aerosols: effects on aerosol optical properties and surface radiation levels. *Atmos. Chem. Phys*. 7: 4257–4266.

Balasubramanian, R., Gao, X., Hatakeyama, S., Hwang, J. and Tsai, C.J. (2017). Overview of the special issue "$PM_{2.5}$ in Aisa" for 2015 asian aerosol conference. *Aerosol Air Qual. Res.* 17: 351–355.

Bond, T.C., Streets, D.G., Yarber, K.F., Nelson, S.M., Woo, J.H. and Klimont, Z. (2004). A technology-based global inventory of black and organic carbon emissions from combustion. *J. Geophys. Res. Atmos.* 109 (D14).

Cao, G., Zhang, X., Wang, Y. and Zheng, F. (2008). Estimation of emissions from field burning of crop straw in China. *Chin. Sci. Bull.* 53: 784–790.

Chen, L., Shi, M.S., Li, S.H., Gao, S., Zhang, H., Sun, Y.L., Mao, J., Bai, Z.P., Wang, Z.L. and Zhou, J. (2017). Quantifying public health benefits of environmental strategy of $PM_{2.5}$ air quality management in Beijing-Tianjin-Hebei region, China. *J. Environ. Sci.* 57:33–40.

Duan, F., Yu, L.T. and Cachier, H. (2004). Identification and estimate of biomass burning contribution to the urban aerosol organic carbon concentrations in Beijing. *Atmos. Environ*. 28:1275–1282.

ACCEPTED MANUSCRIPT

Eckhardt, S., Breivik, K., Manø, S. and Stohl, A. (2007). Record high peaks in PCB concentrations in the Arctic atmosphere due to long-range transport of biomass burning emissions. *Atmos. Chem. Phys.* 7:4527–4536.

Emilsson, S., 2006. International Handbook—From extraction of forest fuels to ash recycling. *Stockholm: Swedish Forest Agency, Jönköping.*

Engling, G., He, J, Betha, R. and Balasubramanian, R. (2014). Assessing the regional impact n Indonesian biomass burning emissions based on organic molecular tracers and chemical mass balance modeling. *Atmos. Chem. Phys.* 14:2773–2798.

Habeebullah, T.M.A. (2016). Chemical composition of particulate matters in Makkah-focusing on cations, anions and heavy metals. *Aerosol Air Qual. Res.* 16: 336–347.

Hao, C.M., Chen, Y.J., Li, R.M. and He, X.W. (2009). The soil heavy metal pollution evaluation of Pinghu based on geochemical standardization method. *Environ. Pollut. Control* 32:96–99. (in Chinese)

Hasan, M., Salam, A. and Alam, A.M.S. (2009). Identification and characterization of trace metals in black solid materials deposited from biomass burning at the cooking stoves in Bangladesh. *Biomass Bioenerg.* 33:1376–1380.

Huang, X., Li, M.M., Hans, R.F., Song, Y., Di, C. and Lei, Z. (2012). Mercury emissions from biomass burning in China. *Environ. Sci. Technol*. 45:9442–9448.

Kondo, Y., Matsui, H., Moteki, N., Sahu, L., Takegawa, N., Kajino, M., Zhao, Y., Cubison, M.J., Jimenez, J.L., Vay, S., Diskin, G.S., Anderson, B., Wisthaler, A., Mikoviny, T., Fuelberg, H.E., Blake, D.R., Huey, G., Weinheimer, A.J., Knapp, D.J. and Brune, W.H. (2011). Emissions of black carbon, organic, and inorganic aerosols from biomass burning in North America and Aisa in 2008. *J. Geophys. Res.* 116:D08204.

Kong, S.F., Shi, J.W., Lu, B., Qiu, W.G., Zhang, B.S., Peng, Y., Zhang, B.W. and Bai, Z.P. (2011). Characterization of PAHs within PM_{10} fraction for ashes from coke production, iron smelt, heating station and power plant stacks in Liaoning province, China. *Atmos. Environ*. 45:3777–3785.

Lanzerstorfer, C. (2015). Chemical composition and physical properties of filter fly ashes from eight grate-fired biomass combustion plants. *J. Environ. Sci.* 30:191–197.

Lee, C.T., Ram, S.S., Nguyen, D.L., Chou, C.C.K., Chang, S.Y., Lin, N.H., Chang, S.C., Hsiao, T.C., Sheu, G.R., Ou-Yang, C.F., Chi, K.H., Wang, S.H. and Wu, X.C. (2016). Aerosol chemical profile of near-source biomass burning smoke in Sonala, Vietnam during 7-SEAS campaigns in 2012 and 2013. *Aerosol Air Qual. Res.* 16: 2603–2617.

Li, J.X., Li, P.R., Yuan, L., Yin, Y., Wang, Z.Z., Li, J., Li, Y.N., Ren, G. and Cai, Z.X. (2017). Physical and optical properties of atmospheric aerosols in summer at a suburban site in North China. *Aerosol Air Qual. Res.* 17: 1374–1388.

Li, P.H., Kong, S.F., Geng, C.M., Han, B., Lu, B., Sun, R.F., Zhao, R.J. and Bai, Z.P. (2013). Assessing the hazardous risks of vehicle inspection workers' exposure to particulate heavy metals in their work places. *Aerosol Air Qual. Res*. 13: 255–265.

Li, Z.Y., Chen, L., Liu, S.T., Ma, H.Q., Wang, L., An, C.X. and Zhang, R.L. (2016). Characterization of PAHs and PCBs in fly ashes of eighteen coal-fired power plants. *Aerosol Air Qual. Res.* 16:3175–3186.

Li, Z.Y., Ji, Y.Q., Ma, H.Q., Zhao, P., Zeng, X.C., Liu, S.T., Jiang, Y.J., Wang, L., Liu, A.Q., Gao, H.Y., Liu, F.D. and Mwangi, J.K. (2017). Characterization of inorganic elements within $PM_{2.5}$ and PM_{10} fractions of Fly Ashes from Coal-Fired Power Plants. *Aerosol Air Qual. Res.* 17: 1105–1116.

ACCEPTED MANUSCRIPT

Liu, X., Gu, J., Li, Y., Cheng, Y., Qu, Y., Han, T., Wang, J., Tian, H., Chen, J. and Zhang, Y. (2013). Increase of aerosol scattering by hygroscopic growth: Observation, modeling, and implications on atmospheric visibility. *Atmos. Res.* 132–133: 91–101.

Oanh, N.T.K., Tipayarom, A., Bich, T.L., Tipayarom, D., Simpson, C.D., Hardie, D. and Liu, L.J.S. (2015). Characterization of gaseous and semi-volatile organic compounds emitted from field burning of rice straw. *Atmos. Environ.* 119:182–191.

Ommi, A., Emami, F., Zíková, N., Hopke, P.K. and Begum, B.A. (2017). Trajectory-based models and remote sensing for biomass burning assessment in Bangladesh. *Aerosol Air Qual. Res.* 17: 465–475.

Popovicheva, O.B., Kozlov, V.S., Engling, G., Diapouli, E., Persiantseva, N.M., Timofeev, M.A., Fan, T.S., Saraga, D. and Eleftheriadis, K. (2015). Small-scale study of Siberian biomass burning: I. Smoke microstructure. *Aerosol Air Qual. Res*. 15: 117–128.

Saqib, N. and Bäckström, M. (2016). Chemical association and mobility of trace elements in 13 different fuel incineration bottom ashes. *Fuel* 172: 105–117.

Shi, Y. S. and Yamaguchi, Y. (2014). A high−resolution and multi−year emissions inventory for biomass burning in Southeast Asia during 2001−2010. *Atmos. Environ*. 98: 8−16.

Sigler, J.M., Lee, X. and Munger W. (2003). Emission and long-range transport of gaseous mercury from a large-scale Canadian boreal forest fire. *Environ. Sci. Technol*. 37: 4343–4347.

Stupak, I., Asikainen, A., Röser, D. and Pasanen, K. (2014). Review of recommendations for forest energy harvesting and wood ash recycling. *Springer Netherlands,* 12:155–196.

Tian, J., Chow, J.C., Cao, J., Han, Y., Ni, H., Chen, L.W.A., Wang, X., Huang, R., Moosmüller, H. and Watson, J.G. (2015). A biomass combustion chamber: Design, evaluation, and a case study of wheat straw combustion emission tests. *Aerosol Air Qual. Res*. 15: 2104–2114.

UNDP, United Nations Development Program, World Energy Assessment: Energy and Challenge, *UNDP, New York,* 2002.

Wang, S.X., Wei, W., Du, L., Li, G.H. and Hao, J.M. (2009). Characteristics of gaseous pollutants from biofuel-stoves in rural China. *Atmos. Environ*. 43:4148−4154.

Wang, H., Lou, S., Huang, C., Qiao, L., Tang, X., Chen, C., Zeng, L.M., Wang, Q., Zhou, M. and Lu, S.H. (2014). Source profiles of volatile organic compounds from biomass burning in Yangtze River Delta, China. *Aerosol Air Qual. Res*. 14: 818–828.

Wang, Z.Z, Tan, J.H., Bi, X.H., Duan, J.C., Sheng, G.Y. and Fu, J.M. (2016). Emission characteristics and chemical species from agricultural straw burning smoke. *Environ. Sci. Technol*. 11:150–155. (in Chinese)

Wei, G.X., Liu, H.Q., Zhang, R., Zhu, Y.W. and Xu, X. (2016). Mass concentrations of polychlorinated dibenzo-p-dioxins and dibenzofurans (PCDD/Fs) and heavy metals in different size fractions of hospital solid waste incinerator fly ash particles. *Aerosol Air Qual. Res*. 16: 1569–1578.

Wongphatarakul, V., Friedlander, S.K. and Pinto, J.P. (1998). A comparative study of PM2.5 ambient aerosol chemical databases. *Environ. Sci. Technol*. 32: 3926–3934.

Wotawa, G., De Geer, L.E., Becker, A., Amours, R.D., Jean, M., Servranckx, R. and Ungar, K. (2006). Inter- and intra-continental transport of radioactive cesium released by boreal forest fires. *Geophys. Res. Lett*. 33:L12806.

Zhang, L.H., Xu, H.Z., Yu, Q.C., Li, R.M., Ma, Z.S., Cao, F. and Li, H.L. (2010). The Investigation and Evaluation of the Heavy Metal Pollution in Farmland Soil and Crop in the Qingyuan of Hebei, China. *J. Aro-Environ. Sci.* 29:2139–2146.

Zhang, Z.Z., Wang, W.X., Cheng, M.M., Liu, S.J., Xu, J., He, Y.J. and Meng, F. (2017). The

ACCEPTED MANUSCRIPT

contribution of residential coal combustion to $PM_{2.5}$ pollution over China's Beijing-Tianjin-Hebei region. *Atmos. Environ.* 159:147–161.

Zheng, G., Xu, X., Li, B., Wu, K., Yekeen, T.A. and Huo, X. (2013). Association between Lung Function in School Children and Exposure to Three Transition Metals from an E-Waste Recycling Area. *J. Exposure Anal. Environ. Epidemiol*. 23: 67–72.

Zheng, X.B., Xu, X.J., Yekeen, T.A., Zhang, Y.L., Chen, A.M., Kim, S.S., Dietrich, K.N., Ho, S.M., Lee, S.A., Reponen, T. and Huo, X. (2016). Ambient air heavy metals in $PM_{2.5}$ and potential human health risk assessment in an informal electronic-waste recycling site of China. *Aerosol Air Qual. Res*. 16: 388–397.

Zhou, Y., Xing, X.F., Lang, J.L., Chen, D.S., Cheng, S.Y., Wei, L., Wei, X. and Liu, C. (2017). A comprehensive biomass burning emission inventory with high spatial and temporal resolution in China. *Atmos. Chem. Phys.* 17:2839–2864.

Zhu, H.J., Tao, J., Yan, X.M., Zhou, B.J. and Mwangi, J.K. (2016). Short-term effects of straw application on carbon recycle in a rice-rapeseed rotation system. *Aerosol Air Qual. Res.* 16: 3358–3363.

ACCEPTED MANUSCRIPT

Table Captions

Table 1a–c

Concentration of individual element in BAs with different sizes (μm) from 7 BFs across BTH.

Table 2

CD values for HM profiles between any two sized BA samples within the same BF.

Table 3

CD values for HM profiles among any two out of seven biofuels

ACCEPTED MANUSCRIPT

Table 1a. Concentration of individual element in BAs with different sizes (μm) from 7 BFs across BTH

BF	Size	Si*	Ca*	Mg*	K*	Fe*	Al*	Ti*	Na*	P *	Sr**	Ba**	Mo**	Rb**
	53–67	24.1±3.81	61.5±6.62	14.1±2.81	290±45.1	8.99±1.22	6.42±1.20	1.65±0.96	5.35±1.01	33.0±5.21	189±32.1	128±26.6	13.0±1.25	70.9±5.67
COT	40–53	32.6±4.86	76.1±9.88	19.3±5.21	296±39.9	5.09±1.28	8.18±1.26	1.57±0.82	5.11±1.06	31.1±4.20	213±44.4	188±32.6	13.2±1.23	69.1±4.65
	<40	31.1±5.62	70.5±6.65	14.3±3.88	267±31.1	5.66±1.65	9.16±1.06	1.24±0.65	5.24±1.23	28.7±2.88	255±36.6	155±28.1	14.7±1.06	68.0±4.85
	53–67	179±21.2	56.0±4.44	18.6±6.62	130±25.5	17.9±3.21	15.3±2.85	2.68±0.85	2.89±0.89	15.9±4.51	130±21.1	154±29.0	16.3±2.26	113±25.6
COR	40–53	152±18.9	47.2±9.56	23.5±4.11	134±31.5	17.5±4.16	15.9±3.25	1.69±0.33	2.91±0.65	17.7±4.66	171±28.9	198±28.5	19.0±2.66	114±27.1
	<40	167±41.5	49.1±8.65	21.5±3.22	105±28.7	27.4±8.17	25.9±5.52	2.83±0.64	4.68±0.98	12.3±3.99	176±31.6	260±41.6	23.8±3.11	95.8±19.8
	53–67	179±57.1	155±25.6	4.82±1.05	108±19.8	11.1±1.56	7.49±1.56	1.76±0.25	1.27±0.36	10.0±2.96	97.8±8.61	237±31.0	9.03±1.03	47.6±11.0
MIL	40–53	208±61.2	23.4±3.26	10.9±2.10	148±41.6	6.66±1.85	10.5±3.26	1.15±0.18	1.98±0.54	14.3±3.95	159±25.6	407±32.6	11.7±1.23	65.2±8.96
	<40	227±46.1	21.2±3.25	9.34±1.85	131±39.4	7.82±1.76	18.6±3.16	1.19±0.17	3.22±0.99	13.6±3.65	140±27.6	574±65.5	10.5±1.13	65.8±8.95
	53–67	259±71.1	132±28.1	25.6±5.21	48.7±6.61	13.2±2.16	6.47±1.21	1.66±0.26	1.41±0.42	10.7±2.22	581±75.6	134±11.6	3.17±0.66	54.1±3.26
WAL	40–53	224±33.6	129±48.9	19.9±3.88	51.1±6.66	4.83±1.65	7.30±2.56	0.44±0.11	1.50±0.51	11.2±2.81	545±68.1	121±10.5	3.09±0.75	57.3±9.61
	<40	63.6±5.86	118±22.1	14.3±2.15	42.9±6.21	12.3±3.12	13.1±3.61	0.83±0.22	3.21±0.97	6.92±1.11	490±55.5	163±21.6	2.49±0.36	59.1±8.62
	53–67	159±32.6	256±55.6	11.4±1.85	156±18.5	4.01±1.01	11.7±2.58	0.96±0.09	3.73±1.02	23.8±4.44	219±39.5	200±25.5	12.5±1.41	45.0±7.89
SOR	40–53	159±21.8	255±36.6	9.83±1.95	163±33.6	5.10±1.23	15.7±3.66	0.86±0.16	4.79±1.66	25.1±4.54	237±35.6	234±19.8	14.2±2.34	52.0±11.2
	<40	204±41.1	200±29.9	8.95±0.98	101±26.6	11.4±2.96	30.9±5.85	1.97±0.40	5.56±1.88	14.0±2.26	168±33.3	217±20.0	7.92±1.21	45.1±3.99
	53–67	36.7±3.51	73.3±8.85	68.6±11.2	248±61.2	11.6±3.22	72.8±8.56	1.94±0.56	1.22±0.33	14.7±2.86	980±125	256±26.8	26.5±4.44	155±36.6
SOY	40–53	33.6±2.66	83.8±12.2	74.3±15.1	237±58.9	4.04±1.10	78.5±7.56	0.83±0.15	1.16 ±0.56	13.9±2.11	999±116	283±61.5	26.5±5.66	154±29.9
	<40	79.1±5.87	65.9±8.36	54.7±9.56	210±35.8	7.29±2.51	16.7±3.56	0.92±0.28	1.16±0.56	12.1±1.95	883±105	269±51.5	21.9±5.40	143±28.5
	53–67	63.3±4.26	77.1±10.2	27.6±5.55	284±71.2	4.49±1.02	10.5±2.51	0.81±0.16	2.35±0.76	21.0±3.11	907±95.6	507±102	4.33±0.22	53.9±4.56
SES	40–53	53.8±8.45	73.8±11.1	21.2±3.22	288±75.6	4.59±1.23	12.3±3.25	1.07±0.17	2.45±0.88	20.8±3.01	885±71.5	497±100	3.58±0.33	55.6±5.66
	<40	67.7±8.26	71.8±6.59	19.4±3.91	232±71.0	5.82±1.23	16.1±4.85	0.95±0.16	2.65±0.96	16.9±2.86	808±72.6	529±89.9	2.99±0.18	49.7±3.88

*mg g^{-1}, **μg g^{-1}

ACCEPTED MANUSCRIPT

Table 1b. Concentration of individual element in BAs with different sizes (μm) from 7 BFs across BTH

	Size	Sc**	Li**	Zr**	Y**	Be**	Sb**	Cs**	Ce**	La**	Sm**	W**	Tl***	Bi***
	53–67	1.50±0.12	4.62±0.88	58.8±6.61	2.90±0.25	0.26±0.02	0.69±0.06	0.76±0.06	6.12±0.86	3.24±0.19	0.58±0.06	0.58±0.12	60.0±11.0	100±25.5
COT	40–53	1.69±0.26	4.90±0.96	29.3±4.56	3.05±0.85	0.30±0.01	0.76±0.05	0.79±0.08	7.04±1.01	3.71±0.16	0.61±0.05	0.60±0.08	61.5±12.1	120±30.1
	<40	1.78±0.56	5.39±1.01	19.4±3.55	3.50±1.01	0.37±0.10	0.83±0.10	0.87±0.11	7.91±1.06	4.36±0.55	0.70±0.08	1.23±0.22	74.3±15.0	130±35.2
	53–67	2.88±0.19	8.57±1.08	70.2±15.6	5.74±1.03	0.53±0.12	1.12±0.02	2.40±0.05	17.4±5.16	7.90±1.02	1.30±0.41	0.92±0.11	91.5±11.2	200±51.6
COR	40–53	3.05±0.21	9.19±2.01	68.8±12.6	6.28±0.98	0.64±0.09	1.15±0.11	2.41±0.09	19.4±5.02	8.81±1.15	1.51±0.44	0.99±0.13	130±35.5	210±52.5
	<40	4.35±0.44	9.91±1.96	103±25.6	8.54±0.99	0.81±0.12	1.29±0.13	2.54±0.15	25.7±6.56	13.7±1.85	2.01±0.56	1.05±0.21	140±41.5	290±65.7
	53–67	1.75±0.59	3.52±0.46	86.1±15.5	2.37±0.45	0.22±0.04	0.37±0.06	0.82±0.02	6.67±0.88	3.51±0.66	0.59±0.03	0.46±0.02	120±25.5	140±36.5
MIL	40–53	2.16±0.58	5.77±0.51	34.8±9.87	3.87±0.66	0.32±0.09	0.53±0.09	1.29±0.61	12.1±2.66	5.49±1.06	0.92±0.05	0.48±0.04	220±56.5	150±40.5
	<40	2.87±0.60	7.10±1.08	58.9±11.6	5.39±0.97	0.52±0.10	0.59±0.07	1.61±0.57	16.8±4.08	7.79±1.85	1.38±0.26	0.63±0.05	280±65.5	180±42.0
	53–67	1.02±0.06	3.94±1.00	95.7±19.6	2.07±0.11	0.19±0.05	0.48±0.06	0.57±0.08	5.21±0.56	2.89±0.51	0.47±0.02	0.26±0.01	69.4±15.5	46.5±11.1
WAL	40–53	1.07±0.10	4.44±0.99	23.5±5.89	2.21±0.15	0.22±0.03	0.42±0.04	0.61±0.08	5.44±1.01	2.91±0.46	0.49±0.04	0.31±0.04	75.6±22.5	59.6±15.6
	<40	2.24±0.33	6.56±2.12	29.5±6.15	4.29±0.68	0.40±0.06	0.77±0.07	1.08±0.10	12.5±2.02	5.68±1.00	1.01±0.07	1.00±0.14	150±51.1	86.7±18.9
	53–67	1.97±0.52	7.42±2.11	30.3±5.86	3.72±0.78	0.37±0.08	0.39±0.05	1.07±0.12	11.7±2.06	5.33±0.58	0.93±0.12	0.34±0.02	60.6±18.2	79.8±12.5
SOR	40–53	2.80±0.66	9.64±2.26	36.6±8.65	5.30±1.02	0.45±0.09	0.49±0.07	1.46±0.21	16.4±3.12	7.38±0.98	1.34±0.26	0.47±0.04	77.6±22.0	95.6±15.7
	<40	3.83±1.02	10.3±3.06	67.9±10.5	7.64±0.93	0.75±0.11	0.54±0.05	1.81±0.56	22.4±5.12	11.9±1.56	1.87±0.55	0.51±0.09	120±41.6	110±21.6
	53–67	1.52±0.33	10.4±2.95	89.5±11.5	2.63±0.28	0.21±0.01	0.45±0.03	1.23±0.36	6.05±1.01	3.05±0.44	0.56±0.06	0.39±0.03	110±33.3	54.6±5.85
SOY	40–53	1.65±0.26	11.3±2.86	31.6±9.82	3.04±0.35	0.29±0.05	0.50±0.12	1.31±0.30	6.29±1.26	3.40±0.57	0.63±0.05	0.49±0.05	118±38.8	72.7±12.3
	<40	2.66±0.81	13.8±4.26	34.2±7.66	5.64±0.56	0.54±0.08	0.52±0.11	1.71±0.31	14.2±2.10	6.56±1.04	1.20±0.36	0.60±0.10	210±51.6	100±17.8
	53–67	1.57±0.45	7.62±1.29	33.5±5.64	3.24±0.33	0.28±0.01	0.77±0.13	0.90±0.09	7.14±1.01	3.74±0.52	0.67±0.11	0.86±0.15	51.5±11.2	64.6±8.52
SES	40–53	1.81±0.51	8.17±2.16	23.6±5.02	3.66±0.36	0.33±0.02	0.78±0.15	1.06±0.11	7.61±1.28	3.97±0.66	0.80±0.15	0.88±0.20	67.0±15.6	65.6±7.56
	<40	2.01±0.56	8.78±2.16	28.5±4.99	4.45±0.29	0.35±0.04	0.80±0.22	1.10±0.16	11.3±2.33	5.03±1.08	0.92±0.18	1.01±0.15	70.5±16.8	75.2±9.65

**μg g^{-1}, ***ng g^{-1}

ACCEPTED MANUSCRIPT

Table 1c. Concentration of individual element in BAs with different sizes (μm) from 7 BFs across BTH

	Size	Mn**	Zn**	Cu**	As**	V**	Cr**	Ni**	Co**	Pb**	Sn**	Cd***	Th**	U***
	53–67	386±56.8	192±18.8	69.8±11.8	3.52±0.88	12.6±2.56	9.31±2.58	8.12±2.21	2.96±0.55	16.3±3.66	1.34±0.16	260±59.5	1.14±0.21	280±44.1
COT	40–53	373±45.6	191±19.6	68.8±12.5	3.79±0.78	13.6±2.86	10.2±3.17	8.45±2.61	3.18±0.75	17.0±3.98	1.54±0.26	270±68.1	1.20±0.25	300±46.4
	<40	360±50.1	192±21.5	65.8±15.8	3.84±0.66	15.9±3.15	11.9±3.58	8.81±2.87	3.32±1.01	18.7±4.67	4.59±0.76	320±69.5	1.46±0.52	380±52.6
	53–67	565±88.9	428±71.2	64.0±18.0	3.47±0.52	57.2±6.51	25.3±5.62	11.2±2.95	4.81±1.21	28.3±5.26	0.99±0.15	580±89.1	2.47±0.34	550±61.1
COR	40–53	624±91.2	456±65.6	66.2±20.1	3.80±0.75	79.3±7.16	35.9±6.88	12.2±3.01	5.38±1.26	25.3±4.11	2.90±0.27	600±92.5	2.76±0.43	640±66.4
	<40	635±91.6	369±55.5	70.0±22.6	4.44±0.36	81.1±9.15	45.6±8.21	16.6±4.01	7.29±2.31	22.2±3.88	2.98±0.75	610±85.6	3.63±0.81	810±78.6
	53–67	338±36.6	178±15.5	19.9±3.56	1.93±0.27	11.2±1.95	8.54±1.79	6.09±1.55	3.02±0.87	13.2±4.10	1.09±0.25	380±62.1	1.17±0.20	180±58.1
MIL	40–53	481±45.6	233±21.9	30.1±5.52	2.22±0.29	16.4±3.87	13.2±3.78	9.25±2.51	4.67±1.07	16.5±4.78	1.41±0.41	510±55.2	1.74±0.55	290±62.1
	<40	506±51.2	217±25.9	26.5±7.65	2.69±0.31	22.0±5.78	21.6±3.99	11.2±3.01	5.10±2.11	17.4±5.21	1.58±0.51	530±67.1	2.38±0.88	400±91.6
	53–67	502±52.5	200±33.3	48.1±7.81	2.62±0.18	6.03±1.02	6.64±1.26	8.20±2.12	2.04±0.36	6.35±1.26	0.91±0.26	61.5±6.22	0.98±0.12	210±33.3
WAL	40–53	545±60.1	205±27.2	51.7±7.99	2.83±0.24	6.61±1.11	8.03±2.11	9.19±3.13	2.32±0.39	6.69±2.10	0.99±0.21	69.6±7.25	1.13±0.27	260±36.6
	<40	460±40.1	164±21.8	40.1±5.61	3.23±0.36	16.5±3.25	18.9±5.11	14.4±4.44	3.97±0.66	8.86±2.36	1.17±0.31	130±12.8	1.98±0.38	380±55.1
	53–67	320±29.8	153±21.5	46.2±6.62	2.23±0.10	14.6±3.40	25.8±1.78	7.16±1.87	2.62±0.67	8.47±2.65	0.98±0.27	280±22.5	1.72±0.71	400±67.5
SOR	40–53	375±32.6	164±23.5	49.7±7.95	3.52±0.12	20.8±4.31	37.9±3.61	9.09±2.27	3.46±1.03	10.3±3.12	1.35±0.41	310±38.1	2.37±0.66	530±76.5
	<40	320±35.5	121±27.6	31.3±3.65	3.68±0.11	27.1±5.89	43.5±4.58	11.8±3.02	4.46±1.65	9.39±3.56	1.38±0.44	410±42.6	3.03±0.99	700±101
	53–67	528±55.6	118±15.2	163±58.8	2.30±0.09	7.66±1.26	6.86±1.36	6.31±1.22	2.34±0.41	4.27±0.65	1.07±0.22	77.1±6.81	1.23±0.31	420±56.7
SOY	40–53	511±51.6	121±18.2	163±60.8	2.69±0.08	11.7±2.55	8.16±2.16	6.91±1.65	2.51±0.55	4.64±0.78	1.09±0.37	97.2±8.21	1.24±0.25	460±69.9
	<40	539±52.1	137±25.7	142±44.4	2.82±0.11	20.2±4.56	19.3±3.66	11.1±2.64	3.79±0.86	7.68±1.78	1.48±0.38	120±16.2	2.15±0.44	600±75.5
	53–67	276±25.1	281±33.4	146±45.9	1.87±0.06	12.2±2.87	8.34±2.12	9.50±2.82	2.15±0.16	5.10±1.85	1.66±0.58	66.3±5.16	1.27±0.41	410±58.3
SES	40–53	283±26.8	290±36.9	152±48.2	2.07±0.05	14.8±2.78	9.85±3.25	10.3±2.95	2.45±0.52	6.00±2.01	1.68±0.61	73.6±6.35	1.33±0.55	430±66.4
	<40	261±31.5	300±25.8	180±33.6	2.83±0.10	16.1±3.33	10.9±3.65	11.5±2.80	2.74±0.78	6.82±2.51	1.72±0.62	78.2±9.15	1.74±0.51	450±70.5

reported in μg g^{-1}, * reported in ng g^{-1}

ACCEPTED MANUSCRIPT

Table 2. CD values for HM profiles between any two sized BA samples within the same BF

BF	Bottom ash	CD value	BF	Bottom ash	CD value
	$PM_{53–67}$ *vs* $PM_{40–53}$	0.025±0.015		$PM_{53–67}$ *vs* $PM_{40–53}$	0.134±0.015
COT	$PM_{53–67}$ *vs* $PM_{–40}$	0.186±0.058	SOR	$PM_{53–67}$ *vs* $PM_{–40}$	0.205±0.024
	PM_{40} *vs* $PM_{40–53}$	0.178±0.032		PM_{40} *vs* $PM_{40–53}$	0.131±0.021
	$PM_{53–67}$ *vs* $PM_{40–53}$	0.155±0.021		$PM_{53–67}$ *vs* $PM_{40–53}$	0.082±0.009
COR	$PM_{53–67}$ *vs* $PM_{–40}$	0.197±0.023	SOY	$PM_{53–67}$ *vs* $PM_{–40}$	0.256±0.038
	PM_{40} *vs* $PM_{40–53}$	0.115±0.032		PM_{40} *vs* $PM_{40–53}$	0.214±0.028
	$PM_{53–67}$ *vs* $PM_{40–53}$	0.069±0.011		$PM_{53–67}$ *vs* $PM_{40–53}$	0.056±0.005
MIL	$PM_{53–67}$ *vs* $PM_{–40}$	0.141±0.031	SES	$PM_{53–67}$ *vs* $PM_{–40}$	0.113±0.012
	PM_{40} *vs* $PM_{40–53}$	0.095±0.008		PM_{40} *vs* $PM_{40–53}$	0.065±0.004
	$PM_{53–67}$ *vs* $PM_{40–53}$	0.081±0.010			
WAL	$PM_{53–67}$ *vs* $PM_{–40}$	0.259±0.012			
	PM_{40} *vs* $PM_{40–53}$	0.221±0.021			

ACCEPTED MANUSCRIPT

Table 3. CD values for HM profiles among any two out of seven biofuels

Biofuel	CD value	Biofuel	CD value
COT *vs* COR	0.280±0.005	MIL *vs* WAL	0.278±0.033
COT *vs* MIL	0.212±0.014	MIL *vs* SOR	0.153±0.023
COT *vs* WAL	0.246±0.017	MIL *vs* SOY	**0.371**±0.045
COT *vs* SOR	0.185±0.044	MIL *vs* SES	**0.380**±0.066
COT *vs* SOY	0.288±0.055	WAL *vs* SOR	0.248±0.034
COT *vs* SES	0.294±0.012	WAL *vs* SOY	0.297±0.056
COR *vs* MIL	0.250±0.022	WAL *vs* SES	**0.359**±0.068
COR *vs* WAL	0.279±0.043	SOR *vs* SOY	0.279±0.020
COR *vs* SOR	0.278±0.026	SOR *vs* SES	**0.341**±0.019
COR *vs* SOY	**0.467**±0.067	SOY *vs* SES	0.177±0.023
COR *vs* SES	**0.462**±0.071		

The bold numbers were higher than 0.3

ACCEPTED MANUSCRIPT

Figure Captions

Fig. 1.

Sampling map for bottom ashes from biomass burning.

Fig. 2.

Bottom ash yields for 7 BFs, a) Size distribution of BA yields for 7 BFs, b) Mean values of BA yields for 7 BFs.

Fig. 3.

a) The Σ_{39}IEs for different sized BAs from 7 BFs, b) Relationship between Σ_{39}IEs and Σ_{8}TEs.

Fig. 4.

Enrichment factors of 12 heavy metals in different sized BAs from 7 BFs.

ACCEPTED MANUSCRIPT

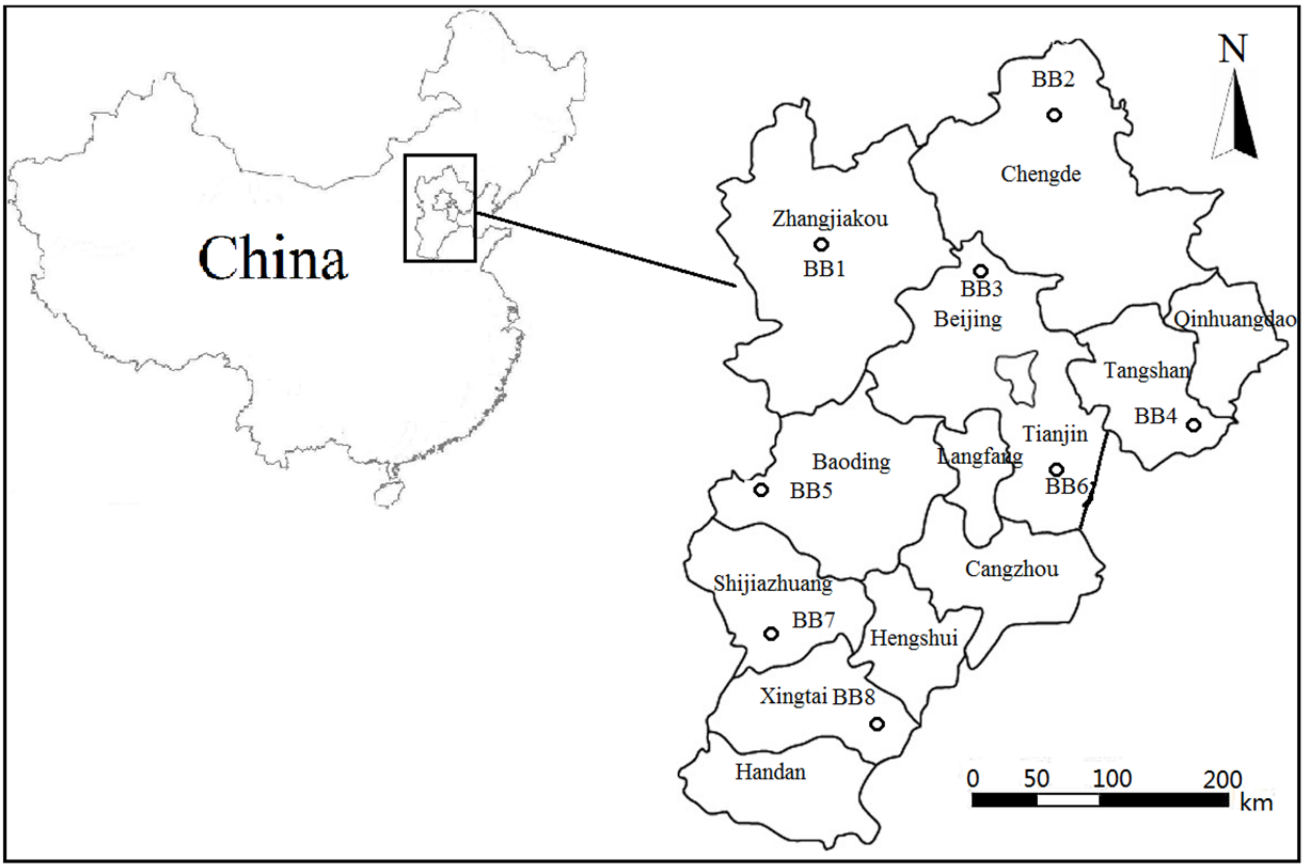

Fig. 1. Sampling map for bottom ashes from biomass burning

ACCEPTED M

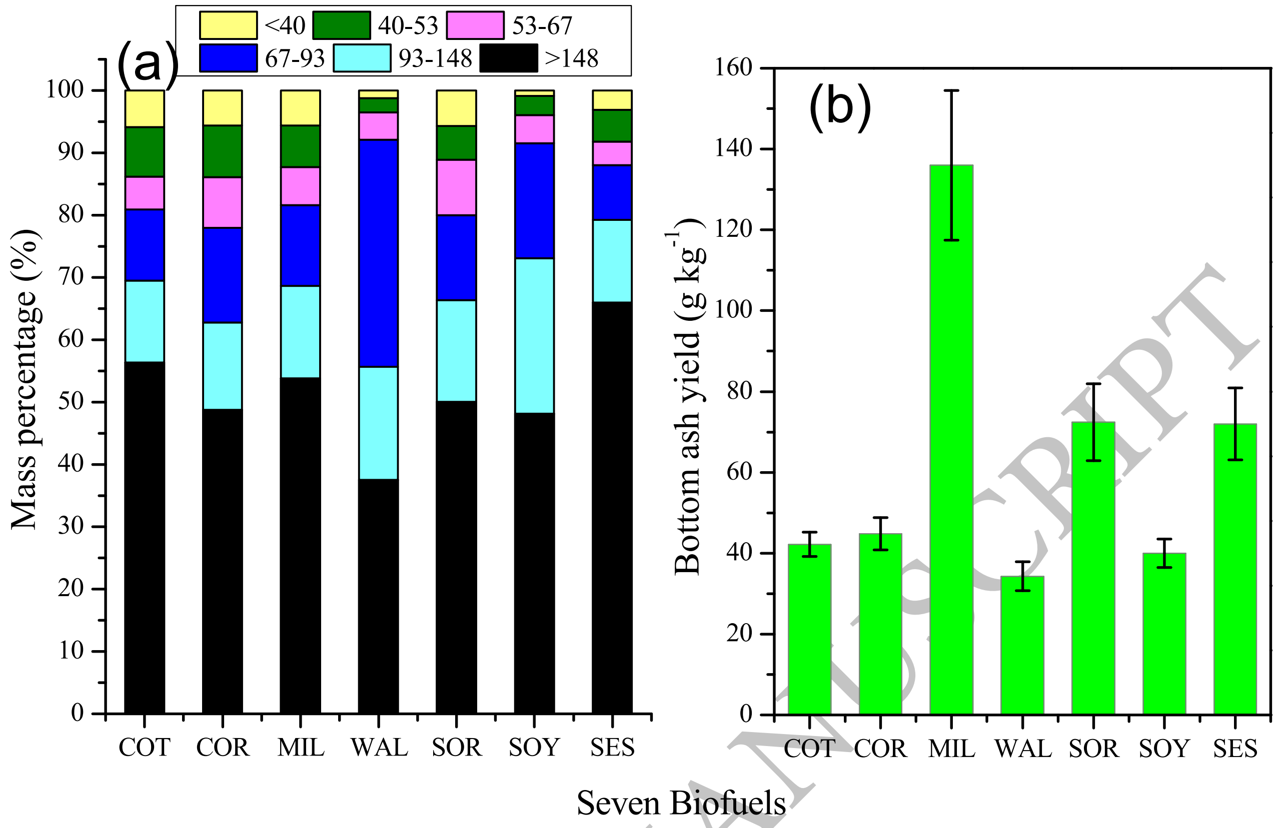

Fig. 2. Bottom ash yields for 7 BFs, a) Size distribution of BA yields for 7 BFs; b) Mean values of BA yields for 7 BFs.

ACCEPTED MANUSCRIPT

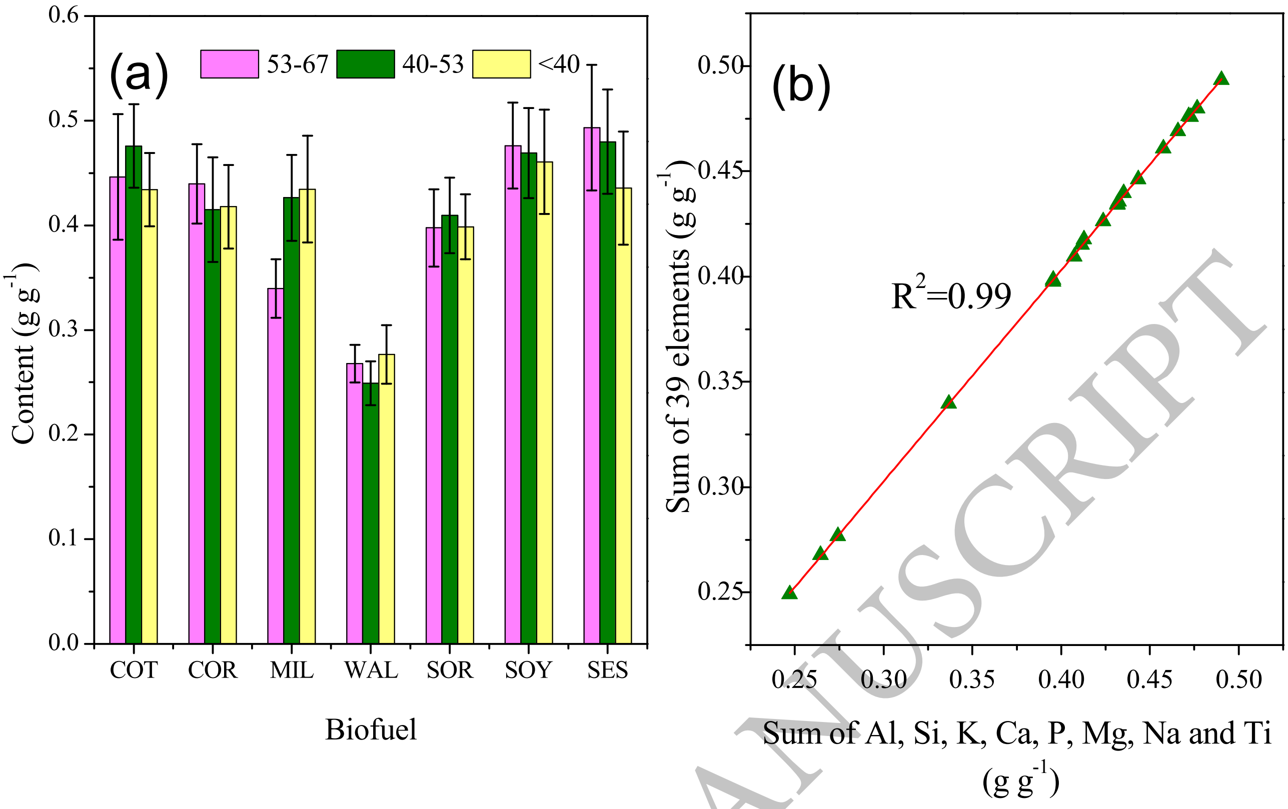

Fig. 3. a) The Σ_{39}IEs for different sized BAs from 7 BFs, b) Relationship between Σ_{39}IEs and Σ_8TEs.

ACCEPTED MANUSCRIPT

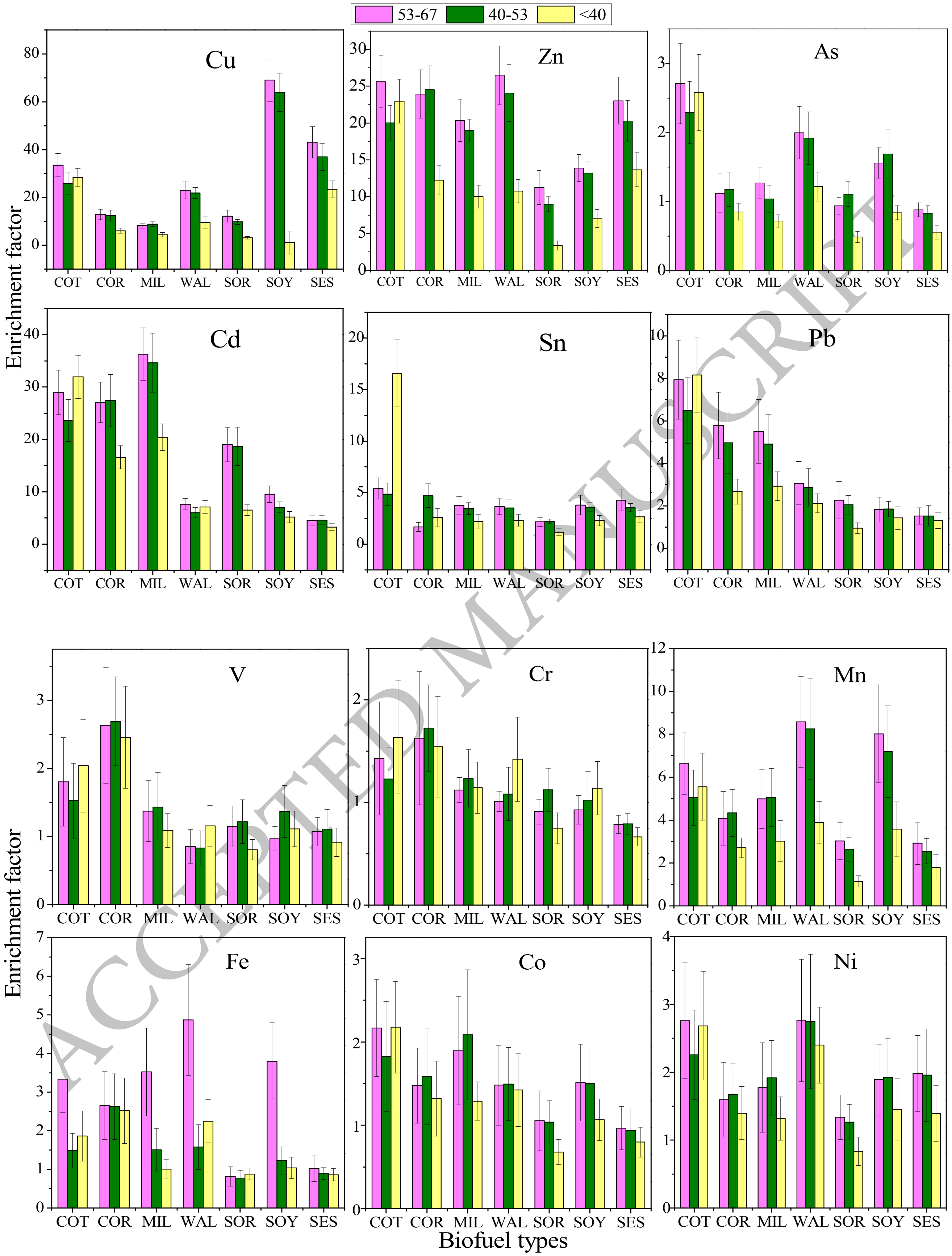

Fig. 4. Enrichment factors of 12 heavy metals in different sized BAs from 7 BFs.

ACCEPTED MANUSCRIPT